Thermal responses in global marine planktonic food webs mediated through temperature effects on metabolism

Kevin Archibald[1], Stephanie Dutkiewicz[2,3], Charlotte Laufkötter[4,5], and Holly V. Moeller[1]

[1]Department of Ecology, Evolution, and Marine Biology. University of California Santa Barbara, Santa Barbara, CA, USA
[2]Department of Earth, Atmospheric, and Planetary Sciences, Massachusetts Institute of Technology, Cambridge, MA, USA
[3]Center for Global Change Science, Massachusetts Institute of Technology, Cambridge, MA, USA
[4]Climate and Environmental Physics, University of Bern, Switzerland
[5]Oeschger Centre for Climate Change Research, University of Bern, Switzerland

Key Points:

- Anthropogenic warming increases metabolic rates; when considered in isolation, it can increase global marine primary productivity.
- However, transient increases in export lead to decreased phytoplankton and zooplankton biomass following ecosystem warming.
- When heterotrophic processes are more sensitive to temperature than photosynthesis, these changes are magnified.

Corresponding author: Kevin Archibald, karchibald@ucsb.edu

Abstract

Rising ocean temperatures affect marine microbial ecosystems directly, since metabolic rates (e.g. photosynthesis, respiration) are temperature-dependent, but temperature also has indirect effects mediated through changes to the physical environment. Empirical observations of the long-term trends in biomass and productivity measure the integrated response of these two kinds of effects, making the independent components difficult to disentangle. We used a combination of modeling approaches to isolate the direct effects of rising temperatures on microbial metabolism and explored the consequences for food web dynamics and global biogeochemistry. We evaluated the effects of temperature sensitivity in two cases: first, that all metabolic processes have the same temperature sensitivity, and alternatively, that heterotrophic processes have higher temperature sensitivity than autotrophic processes. No other study has explored the direct effects of temperature on ecosystem provisioning (primary productivity, biomass, export) independently of the associated changes to the physical environment that result from warming. Microbial ecosystems at higher temperatures are characterized by increased productivity, but decreased biomass stocks as a result of transient, high export events that remove biomass from the surface ocean. Trophic dynamics also mediate changes to community size structure, resulting in longer food chains and increased mean body size at higher temperatures. These ecosystem thermal responses are magnified when the temperature sensitivity of heterotrophs is higher than that of autotrophs. These results provide important context for understanding the combined food web response to direct and indirect temperature effects and inform the construction and interpretation of Earth systems models used in climate projections.

1 Introduction

Over the past century, global average sea surface temperature (SST) has increased by 0.7°C (Bindoff et al., 2007). This surface warming has been accompanied by a steady increase in the heat content of the upper 2000 m of the water column since at least the 1950s, with accelerating trends since 1991 (Cheng et al., 2019). Earth system model projections predict additional increases in SST in the 21st century under all Representative Concentration Pathways (Bopp et al., 2013). In addition to increasing mean conditions, anthropogenic warming has caused unprecedented marine heatwaves in recent years, which are predicted to increase in intensity and frequency (Frölicher et al., 2018; Laufkötter et al., 2020).

Rising ocean temperatures, and corresponding changes in water column structure and circulation, are expected to impact the dynamics of marine planktonic food webs. The relatively short time scale of large spatial scale (e.g. satellite) observations makes it difficult to distinguish between climate-driven trends and natural ecosystem variability (Henson et al., 2010; Dutkiewicz et al., 2019). However, some empirical and modeling studies have indicated changes to phytoplankton biomass and primary productivity. Global phytoplankton biomass has declined by about 1% of the global median value per year since the mid-twentieth century (Boyce et al., 2010) and global net primary productivity (NPP) has been declining since 1999, particularly in lower latitudes (Behrenfeld et al., 2006). Similarly, satellite observations have shown an increase in the extent of marine low-productivity zones since at least 1998, and the rate of expansion of these oligotrophic regions has been increasing in recent years (Polovina et al., 2008; Irwin & Oliver, 2009). Although observational data are still too short-term to definitively establish climate change-driven trends, modeling studies suggest that there are indeed ongoing significant changes occurring in chlorophyll *a*, productivity, and planktonic community structure (Bopp et al., 2005; Dutkiewicz et al., 2015, 2019; Kwiatkowski et al., 2020; Murphy et al., 2020; Benedetti et al., 2021).

Temperature-driven ecosystem changes arise from the cumulative effects of various mechanisms, including direct effects of temperature on the intrinsic biology of marine organisms and indirect effects from changes to the physical environment (Taucher & Oschlies, 2011; Dutkiewicz et al., 2013). Physical drivers of phytoplankton variability include temperature (Behrenfeld et al., 2006; Martinez et al., 2009), water column stratification and the associated reduction in nutrient availability (Falkowski et al., 1998; Behrenfeld et al., 2006; Martinez et al., 2009), and wind (Westerling et al., 2006). Here, we are interested in isolating the direct effects of temperature on planktonic food webs, independent of changes to the physical environment.

Temperature has a direct effect on marine organisms because metabolic processes are intrinsically temperature dependent. At the species level, organisms generally have a temperature optimum at which their growth rate is maximized, but the optimum temperature (and the maximum growth rate achieved at that temperature) varies between species. When the thermal response curves of many species within a functional group are combined, the taxon-level maximum growth rates increase exponentially as a function of temperature. This monotonic relationship between temperature and maximum growth rate is evident in data that integrate growth rates across many species of phytoplankton (Eppley, 1972) or zooplankton (Rose & Caron, 2007). The temperature sensitivity of such groups of species (i.e. the rate of exponential growth of the temperature-metabolic rate curve) can be described using a Q_{10} temperature coefficient following Eppley (1972). Q_{10} is defined as the amount a biological rate (e.g., growth rate) will increase with a temperature increase of 10^oC (discussed more fully below).

Differences may exist in the temperature sensitivity of the growth rates of different planktonic taxa. For example, observational data indicate that heterotrophy may be more sensitive to temperature than phototrophy (López-Urrutia et al., 2006; Rose & Caron, 2007), though the thermodynamic mechanism is not fully understood (Rose & Caron, 2007). As a result, zooplankton growth rates exhibit greater temperature sensitivity than phytoplankton (Rose & Caron, 2007). Recent evidence also demonstrates that temperature sensitivity can vary between phytoplankton functional types, even within taxa with the same metabolic strategy (Anderson et al., 2021). In spite of this, most models that contribute to the Intergovernmental Panel on Climate Change (IPCC) projections have not accounted for differences in temperature sensitivity between taxa, despite evidence that such differences can have important effects on model conclusions (Laufkotter et al., 2015).

Here, we explore the mechanisms by which temperature directly affects marine microbial ecosystem provisioning (e.g. production, biomass, export) and community structure in the absence of indirect effects that accompany warming, including stratification, reduced nutrient supply, and changes to circulation. Within this framework, we also evaluate the effects of alternate assumptions concerning temperature sensitivity: first, that all metabolic rates have the same temperature sensitivity (same Q_{10} values), or that heterotrophic metabolic processes have increased temperature sensitivity (i.e. higher Q_{10} value) compared to autotrophic processes. We utilize a combination of modeling approaches including both global biogeochemical models and simplified heuristic box models simulated under highly idealized warming scenarios.

We find that, as temperature increases, faster metabolic rates drive increased export via the biological pump. Steady-state ecosystems following a temperature increase were characterized by increased productivity, but lower standing biomass of phytoplankton and zooplankton, relative to present day temperature conditions. Warming also causes a shift in community structure, with longer food chains and increased mean body size. Ecosystem-level thermal responses are amplified, and more strongly favor higher trophic levels, when heterotrophy is assumed to have a larger temperature sensitivity than autotrophy.

2 Methods

This study examines the impact of increasing temperature on planktonic food webs. To isolate the direct effects of metabolism on temperature, we used Q_{10} scaling to approximate the relationship between photosynthesis/heterotrophy and temperature. We tested the impacts of this parameterization in two models: The Darwin Model, a global scale ecosystem model that allows us to quantify the impacts of thermal scaling across the world's surface oceans, and a simplified box model, which allows us to isolate specific mechanistic drivers of phenomena observed in Darwin.

2.1 Q_{10} Temperature Coefficients

To estimate the effects of temperature on metabolic rates, we used the same parameterization that is used in climate change simulation models, such as in the IPCC Coupled Model Intercomparison Project (CMIP6; Kwiatkowski et al., 2020). Similar to those models, we quantify the effects of temperature on ecosystem dynamics by parameterizing metabolic rates as exponentially increasing functions of temperature (following Eppley, 1972, Fig. 1). A metabolic rate, R, at a given temperature can be calculated from a known rate, R_0, at reference temperature, T_0, and the Q_{10} temperature coefficient following,

$$R = R_0 Q_{10}^{(T-T_0)/10} \tag{1}$$

This equation assumes that metabolic rates increase monotonically as a function of temperature. Although this is not true of individual species, which have maximum thermal tolerances, here we model *communities* of organisms within a given functional group. Therefore, we have implicitly assumed that whenever a given species passes its thermal maximum, it will be replaced by a different species with a higher temperature range. This monotonic behavior can be seen in data sets that compile maximum growth rates as a function of temperature across many species (e.g. Eppley, 1972; Bissinger et al., 2008). There is evidence that phytoplankton communities near the equator are already nearing their thermal maximum and are therefore more vulnerable to increases in temperature (Thomas et al., 2012). However, we have chosen to simplify our representation of metabolic temperature sensitivity in favor of idealized cases. Importantly, this assumption of monotonicity is how the temperature sensitivity of metabolisms is represented in the IPCC reports (CMIP6; Kwiatkowski et al., 2020) (as well as earlier CMIP models), and so it is useful to do so here so that our results may inform that significant body of work. We investigated two cases of relative temperature sensitivity in autotrophs and heterotrophs (Table 1). First, we assumed that all metabolic processes in the models have the same temperature sensitivity ($Q_{10} = 1.88$). Second, and alternatively, we assumed that heterotrophs have a higher temperature sensitivity (autotrophic Q_{10}=1.88, heterotrophic Q_{10}=2.7).

2.2 Darwin Model

To assess the effects of temperature on the upper ocean ecosystem, we performed simulations using the Darwin model (Fig. 2). The Darwin simulations incorporate a coupled physical/biogeochemical/ecosystem model based on that used in Follett et al. (2022). Circulation and mixing are provided by the Massachusetts Institute of Technology (MIT) general circulation model (MITgcm) (Marshall et al., 1997), constrained to be consistent with altimetric and hydrographic observations (Wunsch & Heimbach, 2007). This three-dimensional global configuration has coarse resolution (1° by 1° horizontally) and 23 depth bins ranging from 10 m in the surface to 500 m at depth. The biogeochemical/ecosystem component captures the cycling of C, N, P, Si, and Fe as they pass through inorganic and (dead and living) organic pools (Dutkiewicz et al., 2015, 2020). The spe-

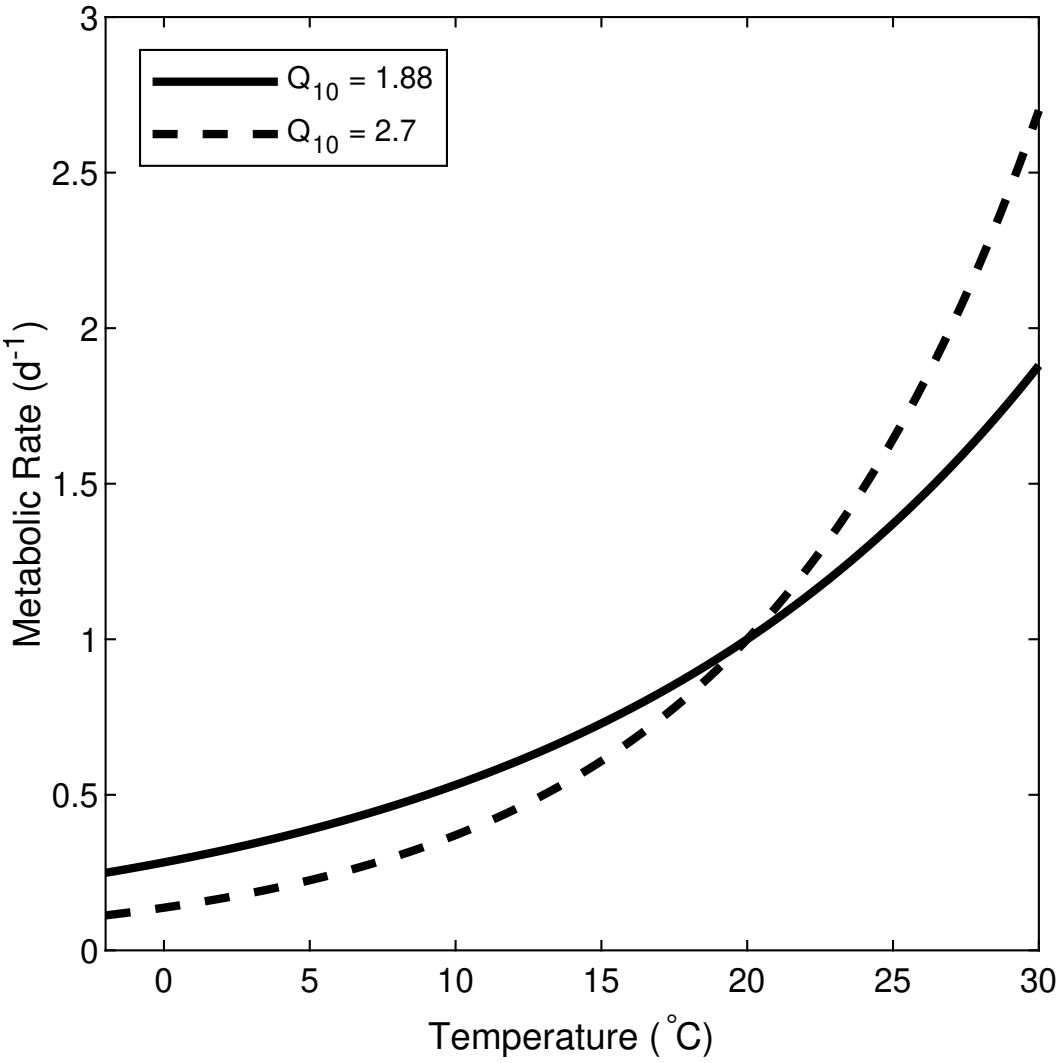

Figure 1. Metabolic rates (e.g. photosynthesis, grazing) as a function of temperature using two different Q_{10} values. See Table 1 for the values used for autotrophic and heterotrophic metabolic processes in different experiments.

cific details of the ecosystem follow from Follett et al. (2022) and resolve 31 phytoplankton (2 picoprokaryotes, 2 picoeukaryotes, 5 coccolithophores, 5 diazotrophs, 9 diatoms, 8 mixotrophic dinoflagellates), 16 zooplankton, and 3 heterotrophic bacteria. Phytoplankton have size resolution spanning from 0.6 μm to 140 μm ESD, zooplankton spanning 4.5 μm to 1,636 μm, and bacteria spanning 0.4 μm to 0.9 μm. Parameters influencing plankton growth, grazing, and sinking are related to size (Dutkiewicz et al., 2020), with specific differences between the six functional groups (Dutkiewicz et al., 2020; Anderson et al., 2021). Phytoplankton growth is limited by multiple nutrients (N, P, Fe, and Si in the case of diatoms) and light (following Geider et al., 1998). Grazing is parameterized using a Holling Type II functional response (Holling, 1965) and is size-specific such that grazers can prey upon plankton 5 to 15 times smaller than themselves, with an optimal size of 10 times smaller (Hansen et al., 1997; Kiørboe, 2018; Schartau et al., 2010). The emergent size distribution of the simulated plankton populations is strongly controlled both by the rate of supply of limiting nutrients (bottom up) and by grazing (top down) (Dutkiewicz et al., 2020; Follett et al., 2022). The output from simulation of Follett et al. (2022) compared well to annual and seasonal observations of chlorophyll-*a*, nutrients, and size and biogeochemical functional group distributions of phytoplankton (Ward, 2015; Buitenhuis et al., 2013). See further discussion in the appendix of Follett et al. (2022).

The only difference between the simulation of Follett et al. (2022) and here is in the treatment of thermal responses of the biological rates. In Follett et al. (2022) phytoplankton growth Q_{10} was based on different functional groups as found in compilation of laboratory experiments in Anderson et al. (2021). Here, instead, we set all phytoplankton growth response to a Q_{10} of 1.88 (following Eppley, 1972), and a Q_{10} of grazing to either 1.88 or 2.7 following Table 1.

To quantify the effects of temperature on ecosystem structure, we ran a series of experiments of 10 year duration, beginning with the same initial conditions (World Ocean Atlas for nutrients, and previous model output for all organic matter). The ecosystem quickly (within approximately 3 years) reaches a quasi-steady state. Here we show results from the 10th year of the simulations. In the series of experiments, the physical circulation and mixing remained identical, but the temperatures that the biological rates experience were altered: in each simulation the temperature was raised at each location, depth, and each time by a specific amount (ΔT=1,3,5 ^{o}C, see Table 1). These experiments are thus highly idealized and designed specifically to interrogate the impact of increasing temperature on biological rates alone. Though there are slight differences in the community composition relative to Follett et al. (2022) given the differences in Q_{10} for plankton growth, the default simulation (i.e. where $\Delta T = 0^o$) compares similarly well to observations of chlorophyll-*a*, nutrients, and size distribution of phytoplankton and functional groups.

2.3 Box Model

To provide mechanistic context to the more complex, dynamical Darwin model, we also employed a simplified box model of the marine food web in the upper ocean (Fig. 3). In this model, the surface ocean is represented as a well-mixed box that contains a single nutrient resource (N), a population of phytoplankton (P), a population of zooplankton (Z), and a pool of detrital organic matter (D). The rate of change of nutrients in the surface ocean depends on the balance between upwelling from the deep ocean, remineralization of detritus, and uptake by phytoplankton. Nutrients are supplied to surface ocean via a fixed upwelling flux, W, and by remineralization of the organic matter with rate r. Nutrients are removed by phytoplankton uptake, which follow Monod dynamics with maximum uptake rate u and half-saturation coefficient k_n,

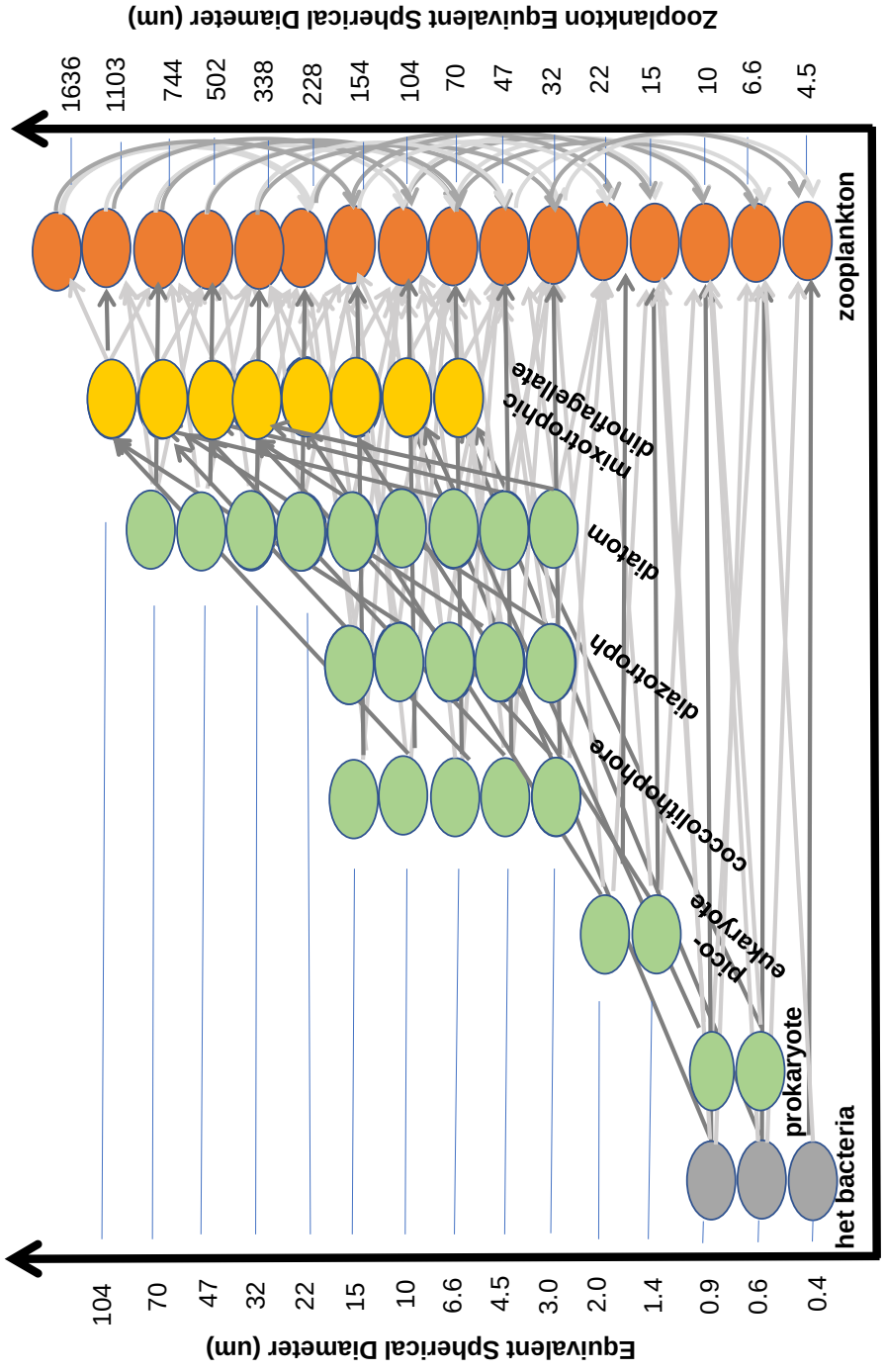

Figure 2. Size classes and functional groups in the Darwin model. The equivalent spherical diameter of each of the 50 resolved plankton types is shown, including bacteria (grey), phytoplankton (green), mixotrophic dinoflagellates (yellow), and zooplankton (orange). Zooplankton are plotted on a separate size axis. The grazing relationships between the different size classes is indicated by arrows, with darker arrows corresponding to higher grazing preference.

Table 1. Summary of Darwin Simulations

Experiment No.	$\Delta T(^{\circ}C)$	Temperature Sensitivity Case	Autotroph Q_{10}	Heterotroph Q_{10}
1	0	Same Q_{10}	1.88	1.88
2	1	Same Q_{10}	1.88	1.88
3	3	Same Q_{10}	1.88	1.88
4	5	Same Q_{10}	1.88	1.88
5	0	Different Q_{10}	1.88	2.7
6	1	Different Q_{10}	1.88	2.7
7	3	Different Q_{10}	1.88	2.7
8	5	Different Q_{10}	1.88	2.7

$$\frac{dN}{dt} = W + rD - \frac{uNP}{k_n + N} \tag{2}$$

Phytoplankton growth is determined by the balance between nutrient uptake and mortality terms. Phytoplankton mortality includes both grazing by zooplankton, which follows Monod dynamics using a maximum grazing rate g and half-saturation coefficient k_p, as well as a quadratic mortality term (ϕ_p) to represent density-dependent loss from outside sources,

$$\frac{dP}{dt} = \frac{uNP}{k_n + N} - \frac{gPZ}{k_p + P} - \phi_p P^2 \tag{3}$$

Zooplankton growth rate is determined by grazing on phytoplankton minus density-dependent mortality at a rate ϕ_z,

$$\frac{dZ}{dt} = \frac{gPZ}{k_p + P} - \phi_z Z^2 \tag{4}$$

Organic matter is added to the detrital pool through phytoplankton and zooplankton mortality, and removed via remineralization and export. The export rate, f, represents the sinking of biogenic particles out of the surface ocean,

$$\frac{dD}{dt} = \phi_p P^2 + \phi_z Z^2 - rD - fD. \tag{5}$$

The model was parameterized to be similar to the Darwin model (Table 2). Temperature dependence was added to the following biological rates: u, g, ϕ_p, ϕ_z, and r, following Eq. (1). We simulated the model under the same two assumptions on Q_{10} between trophic levels: first, we assumed that all rate parameters had the same temperature sensitivity ($Q_{10} = 1.88$), and second, we assumed that the heterotrophic rates (g, phi_p, phi_z) had a higher temperature sensitivity ($Q_{10} = 2.7$). Similar to Darwin model, the results of this box model were examined under different temperature, as well as to consider transient effects.

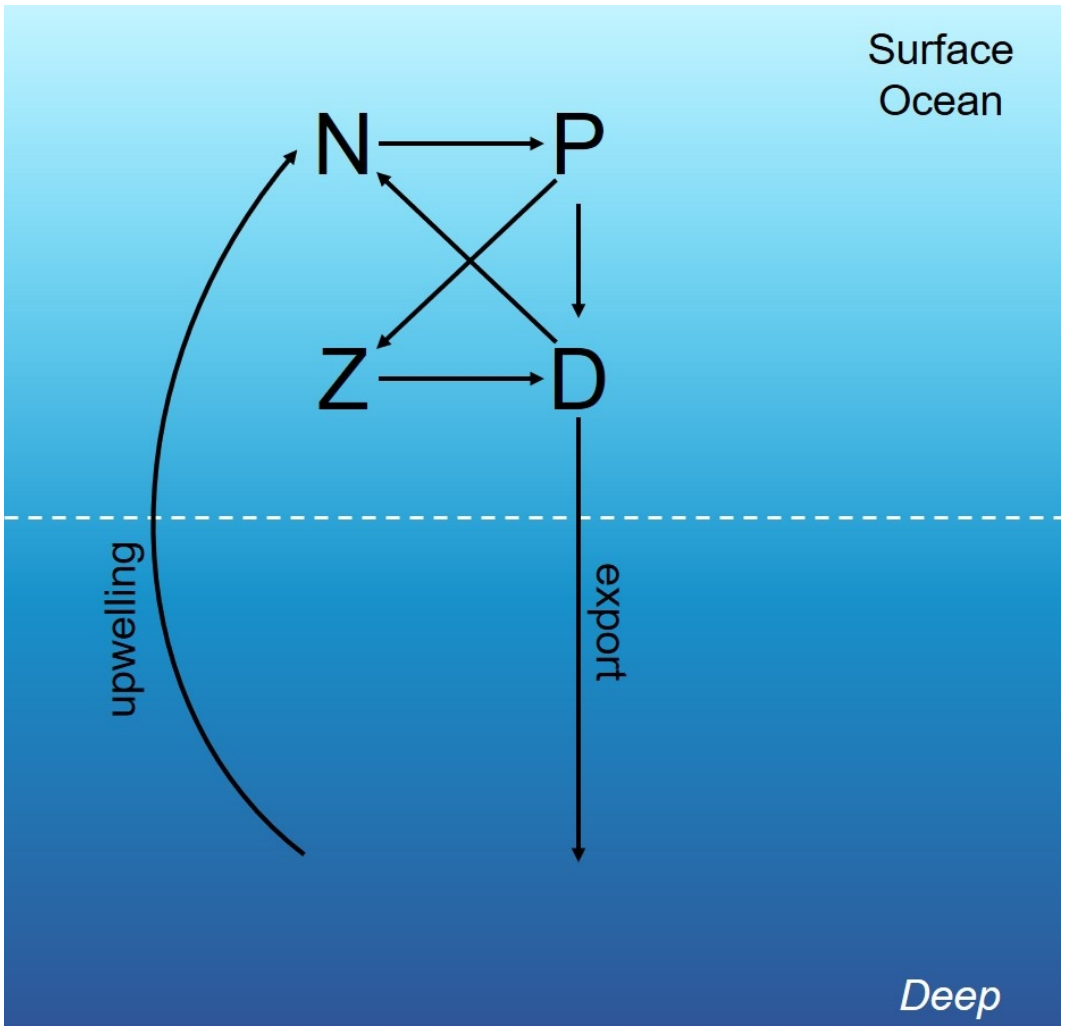

Figure 3. Food Web Box Model. The box model represents the relationships between a nutrient (N), a phytoplankton population (P), a zooplankton population (Z), and a pool of organic matter (D) in the surface ocean. Organic matter is exported out of the surface ocean by a sinking flux and nutrients are supplied back to the surface ocean by upwelling.

Table 2. Model symbols and their meanings

Symbol	Description	Typical Units	Simulation Values
Variables:			
N	inorganic nutrients	$mmol \cdot m^{-3}$	
P	phytoplankton	$mmol \cdot m^{-3}$	
Z	zooplankton	$mmol \cdot m^{-3}$	
D	detritus	$mmol \cdot m^{-3}$	
Parameters:			
u	maximum phytoplankton growth rate	d^{-1}	2.0
k_n	nutrient uptake half-saturation	$mmol \cdot m^{-3}$	0.15
g	maximum zooplankton growth rate	d^{-1}	1.0
k_p	grazing half-saturation	$mmol \cdot m^{-3}$	10
ϕ_p	phytoplankton mortality	d^{-1}	0.01
ϕ_z	zooplankton mortality	d^{-1}	0.1
r	remineralization rate	d^{-1}	0.3
f	export ratio		0.1
w	upwelling flux	$mmol \cdot m^{-3} \cdot d^{-1}$	0.1

3 Results

3.1 Higher temperatures reduce surface ocean planktonic biomass and nutrient availability.

First, we quantified the effects of thermal change on ecosystem provisioning. Globally integrated total NPP increased with temperature in the Darwin model simulations (Fig. 4), following thermal scaling rules. However, biomass of both phytoplankton and zooplankton decreased with temperature (Fig. 4). The direction of the trend with respect to temperature for biomass and productivity was the same for both Q_{10} cases and for different trophic levels, but the magnitude of the thermal response was larger when we assumed that the Q_{10} for heterotrophic metabolic processes was larger than the Q_{10} for autotrophic processes.

More productive ecosystems may contain lower biomass for two reasons: the biomass may have either accumulated in the non-living components of the model (e.g. inorganic nutrients, detritus) or been removed from the surface ocean along export pathways, including the biological pump. To distinguish between compensatory mass redistribution and increased export, we used phosphorus as a mass-conserved tracer, tracking changes in the phosphorus content of inorganic nutrients, phytoplankton and zooplankton size classes, and the detrital pool as temperature increased. Other elements, notably N and Fe, are less useful as a diagnostic due to additional source and loss terms (e.g. aeolian deposition, nitrogen fixation). We observed a small increase in dissolved inorganic phosphate under both temperature sensitivity cases. However, this increase was not enough to compensate for the decrease in phytoplankton and zooplankton biomass. Thus, total upper ocean phosphorus content, which includes both biogenic phosphorus and dissolved phosphate, decreased as temperature increased, providing evidence of a transient increase in export at some point along the trajectory of the simulation (Fig. 5).

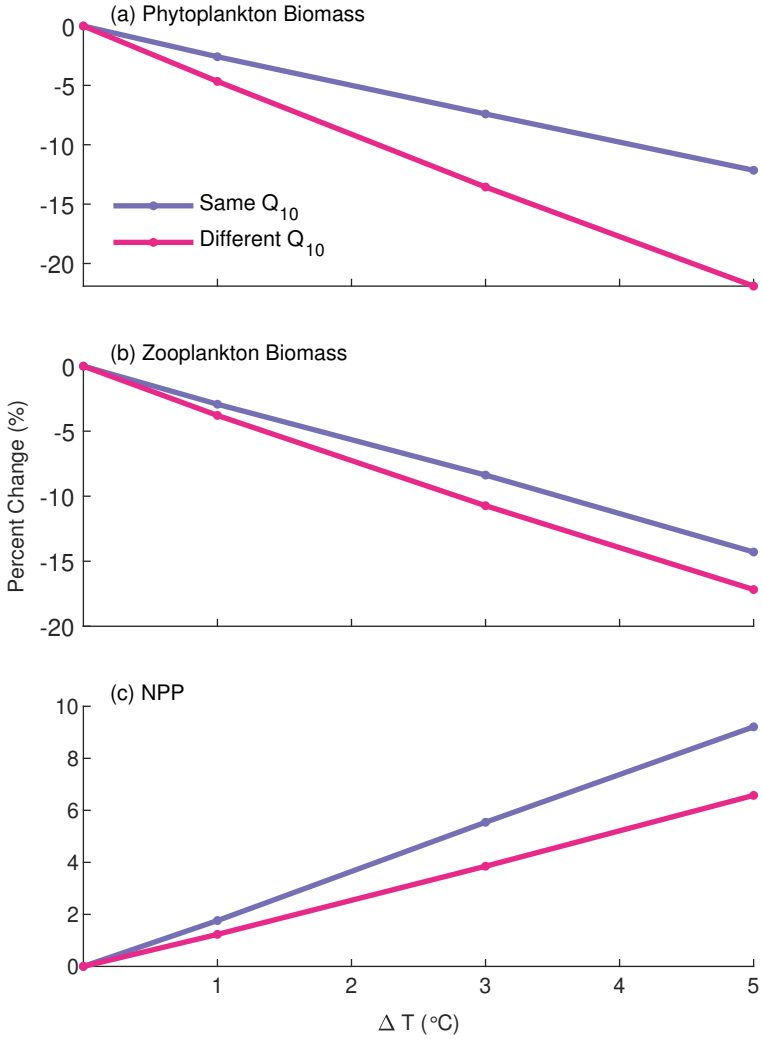

Figure 4. Percent change in globally integrated (a) phytoplankton biomass, (b) zooplankton biomass, and (c) NPP as a function of the increase in temperature relative to historical conditions for both Q_{10} cases.

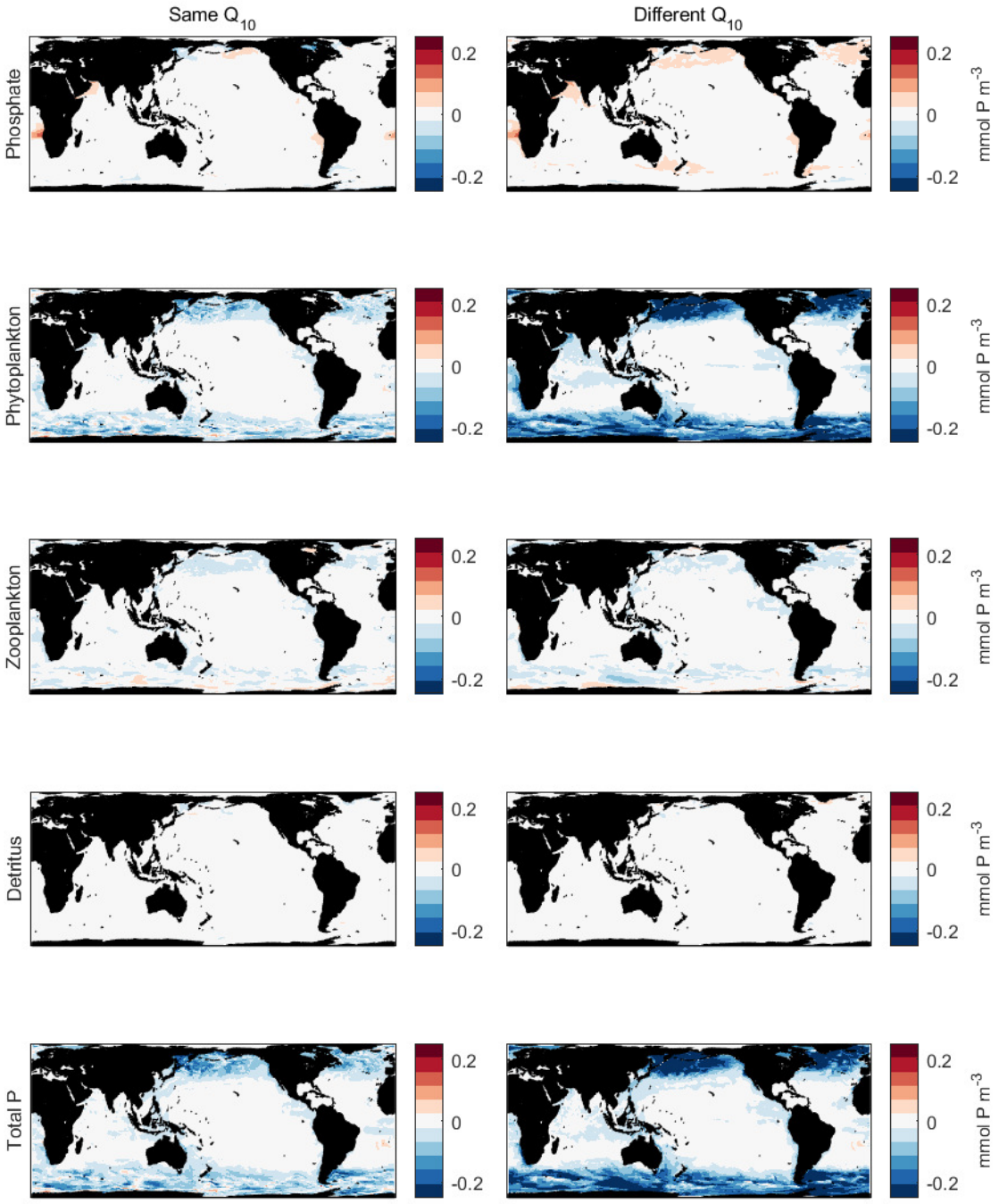

Figure 5. The change in total P content in the surface ocean within different ecosystem components (inorganic phosphate, phytoplankton, zooplankton, and detritus) after a 5 degree temperature increase for both Q_{10} cases.

3.2 Transient increases in export drive biomass and nutrient reductions.

Synthesizing the evidence from the suite of Darwin simulations, we propose the following mechanism for direct temperature effects on marine planktonic food webs (Box 1). Increasing temperature drives higher productivity via accelerating metabolic rates. Increased productivity temporarily results in faster rates of the export of biomass out of the surface ocean along biological pump pathways. Increased export reduces the total mass of P (summed across organic and inorganic pools) in the surface ocean, resulting in a reduction in total biomass. Darwin simulations were conducted for 10 years, so the timescale of interest for this mechanism is both ecologically relevant and small compared to large-scale circulation processes.

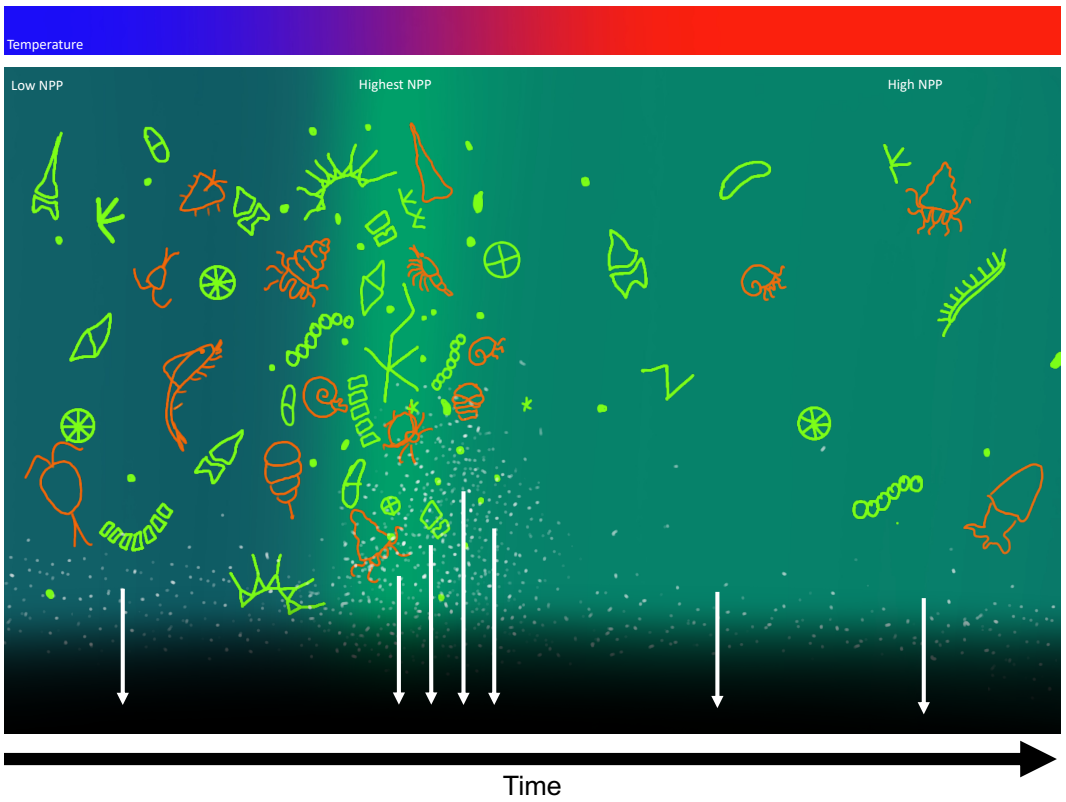

Box 1. In the contemporary ocean (left side), phytoplankton (green) and zooplankton (orange) contribute to export (white arrows) to the deep ocean (black). A hypothetical, acute, and abrupt, increase in temperature causes an acceleration of all metabolic rates, leading to an increase in primary production (light green background) and an increase in biomass of phytoplankton and zooplankton. This increased biomass supports a transient increase in export, which drains nutrients from the surface ocean and causes the system to re-equilibrate at intermediate levels of primary production and lower levels of biomass. (Illustrated by Elise Cypher.)

To provide additional evidence for this proposed mechanism, we turn to the simplified box model of the surface ocean. The transient behavior of the box model plays a key role in establishing the ecosystem thermal response (Fig. 6). The increase in export following an instantaneous temperature perturbation is largely a transient event and declines as overall mass is drained from the surface ocean. NPP, which is a function of both temperature and phytoplankton biomass, also displays a transient peak directly following the temperature increase and slow decline again as the system equilibrates. However equilbrium NPP is still higher than at the lower temperature. Thus, the asymptotic behavior of the model following the temperature change is characterized by increase pro-

ductivity (relative to before the temperature change) and lower biomass of phytoplankton and zooplankton, but the export rate at equilibrium is not significantly increased compared to before the temperature increase. The ecosystem represented in the box model is also more sensitive to temperature when we assume that heterotrophic metabolic processes have a different temperature sensitivity than autotrophic processes (Fig. 7). The temperature-driven decline in equilibrium biomass for both phytoplankton and zooplankton was greater when the zooplankton Q_{10} was larger than the phytoplankton Q_{10}. These results are consistent with the patterns observed in the Darwin simulations.

3.3 Divergent Q_{10} values intensify community structure changes and trophic cascades.

At an aggregate level, increased temperature results in declines in total biomass. However, the Darwin model includes multiple size classes and functional groups, and complex community interaction due to the presence of multiple trophic levels. And while the total biomass summed across all these size classes is inversely related to temperature, trophic dynamics within the food web result in more complicated thermal responses at the scale of individual plankton size classes (Fig. 8). In general, the largest size class that is present in the ecosystem (the highest trophic level) increased at higher temperatures. Increased biomass at the top of the food chain resulted in a trophic cascade, evidenced by an alternating pattern of increasing and decreasing biomass in plankton size classes moving down the food chain (Fig. 8). The trophic cascade effect is somewhat complicated by the effects of competition between plankton functional types and complex grazing relationships that blur the lines between trophic levels, however, the general pattern can be seen across a range of different biogeochemical regimes, including regions with different trophic structure. This is illustrated most clearly by comparing individual size class changes in the Southern and Indian oceans (Fig. 8). Food chains in the Indian ocean are typically longer in the Darwin simulations, with an additional trophic level compared to food chains in the Southern ocean. Consequently, many of the individual plankton size classes show opposite thermal responses.

The net result of all the individual changes to plankton size classes is an increase in the mean body size of the entire plankton community (Fig. 9) and, relatedly, in the biomass-weighted food chain length (Fig. 10) at higher temperatures. These increases were amplified by divergent Q_{10} values for autotrophic and heterotrophic processes. The preference for larger size classes likely arises from a combination of multiple mechanisms, including increased productivity and remineralization rates at higher temperatures that support longer food chains and an increase in carnivores (which tend to be larger-bodied) relative to herbivores and autotrophs. In the box model, we also observed a positive relationship between temperature and the ratio of zooplankton to phytoplankton, lending additional evidence that carnivores at the top of the food chain gain the most advantage from increased productivity.

4 Discussion

The oceans' ecosystems are responding to multiple changes that accompany anthropogenic climate change, including warming, reduced sea-ice, alterations to supply of nutrients, changes to light environment, and ocean acidification. Here we specifically target ecosystem-level changes caused by the direct effect of warming on metabolic rates. Rising ocean temperatures are expected to accelerate the metabolic rates of marine organisms. However, we show that even this relatively simple positive relationship between temperature and metabolic rate does not translate to easily predictable thermal responses at the ecosystem level due to the complicating effects of feedbacks within the food web and interactions with the physical environment. Increased productivity driven by warm-

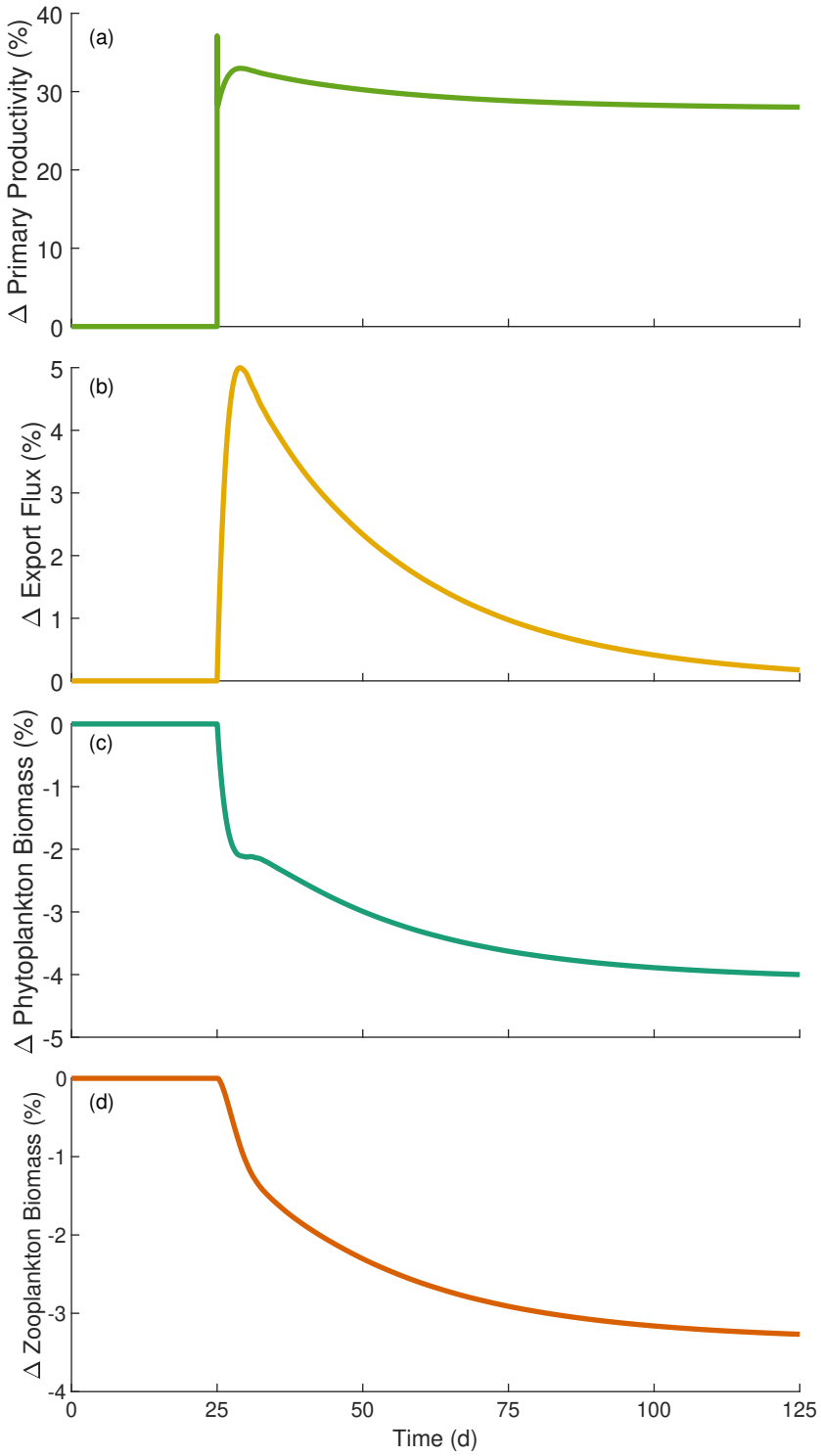

Figure 6. Time series of the box model showing transient behavior in (a) NPP, (b) export, (c) phytoplankton biomass, and (d) zooplankton biomass as the model converges to a new equilibrium following an instantaneous temperature increase of 5 degrees at t = 25.

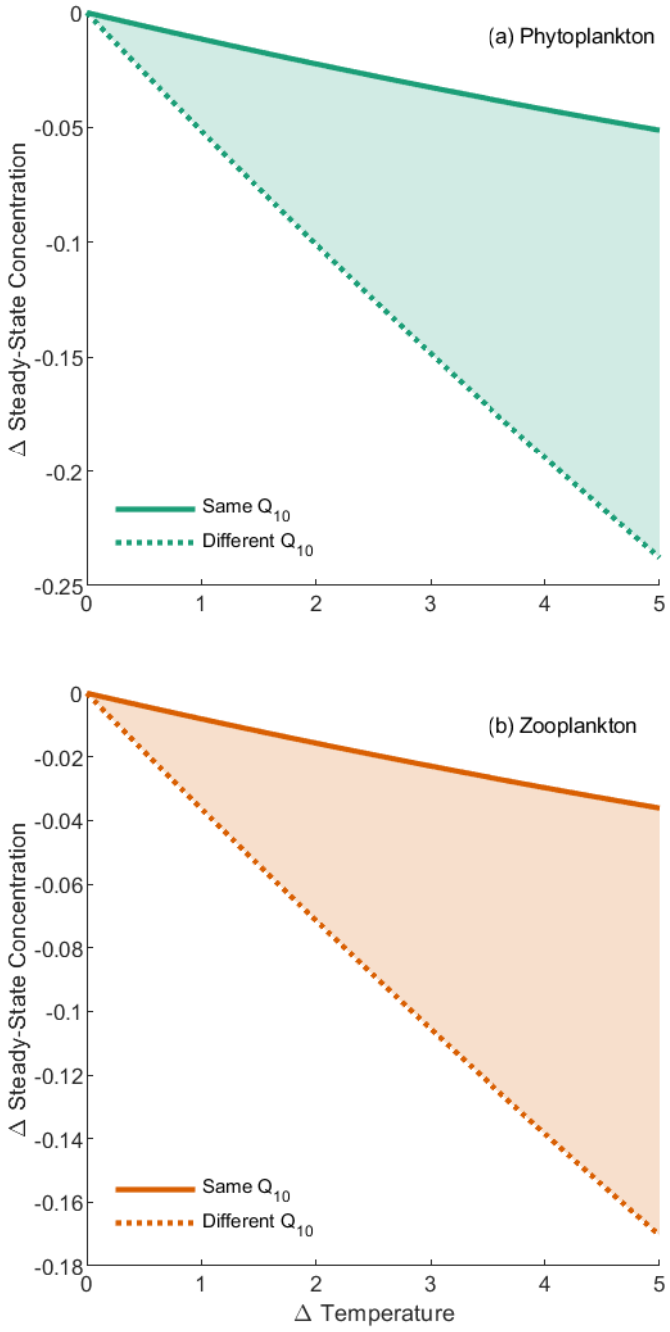

Figure 7. Relative change in the equilibrium (a) phytoplankton and (b) zooplankton biomass as a function of the change in temperature in the box model for both Q_{10} cases

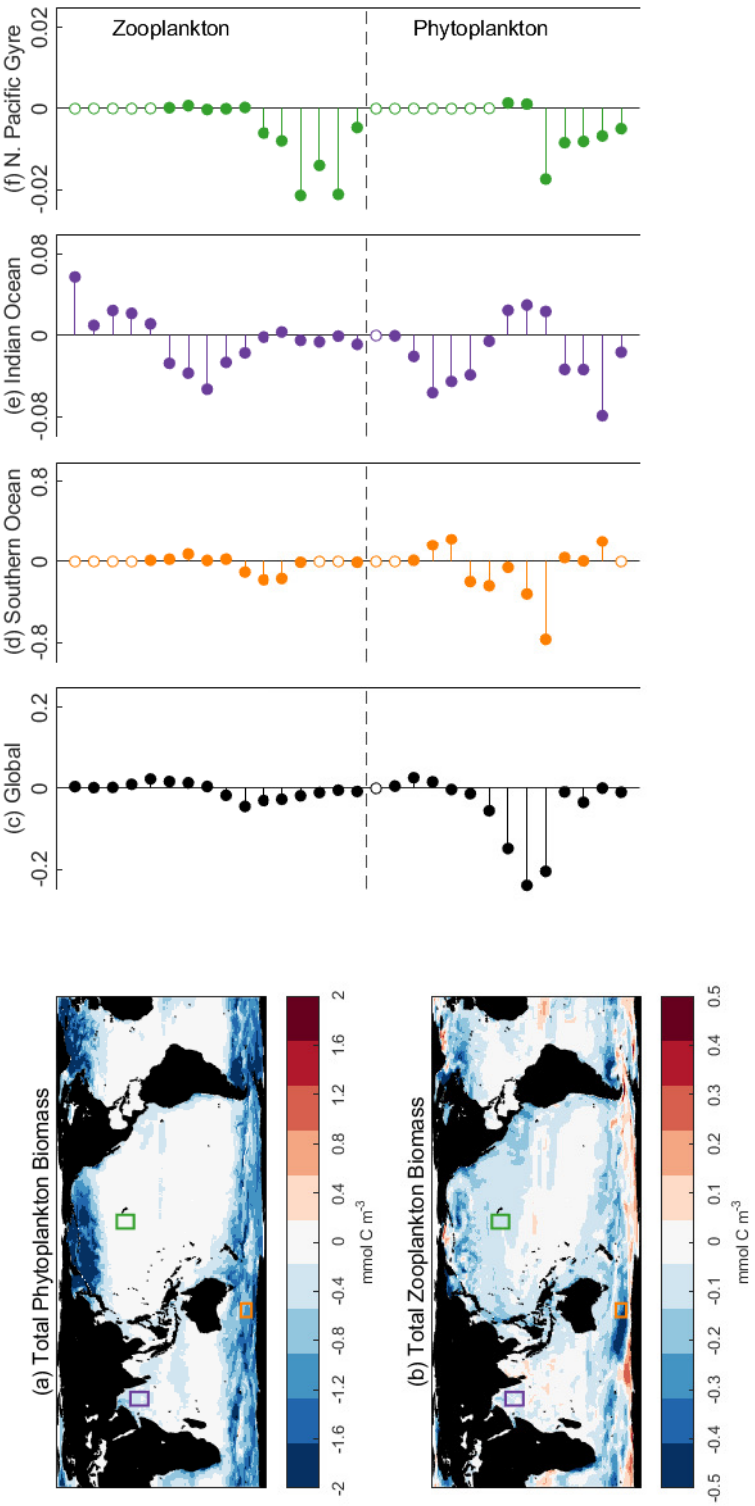

Figure 8. Global distribution of the thermal response in (a) bulk phytoplankton biomass and (b) bulk zooplankton biomass as well size-class specific changes for (c) the global mean, (d) Southern Ocean, (e) Indian Ocean, and (f) the North Pacific gyre. All changes were calculated as the difference in biomass following a 5 degree temperature increase in the different Q_{10} case.

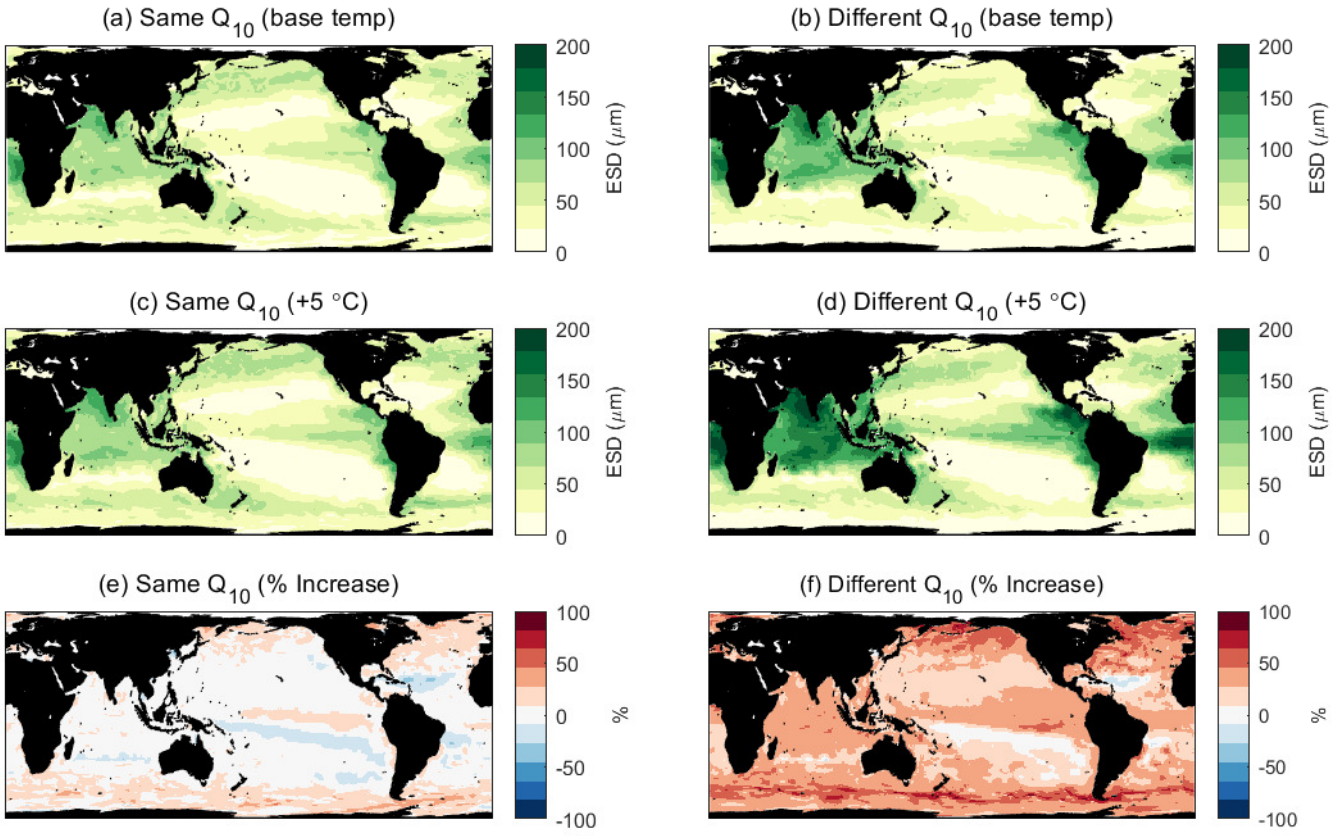

Figure 9. Global distribution of the plankton community mean body size under the base (a,b) and +5 degree (c,d) experiments for both Q_{10} cases and the percent difference (e,f) between the two temperature simulations.

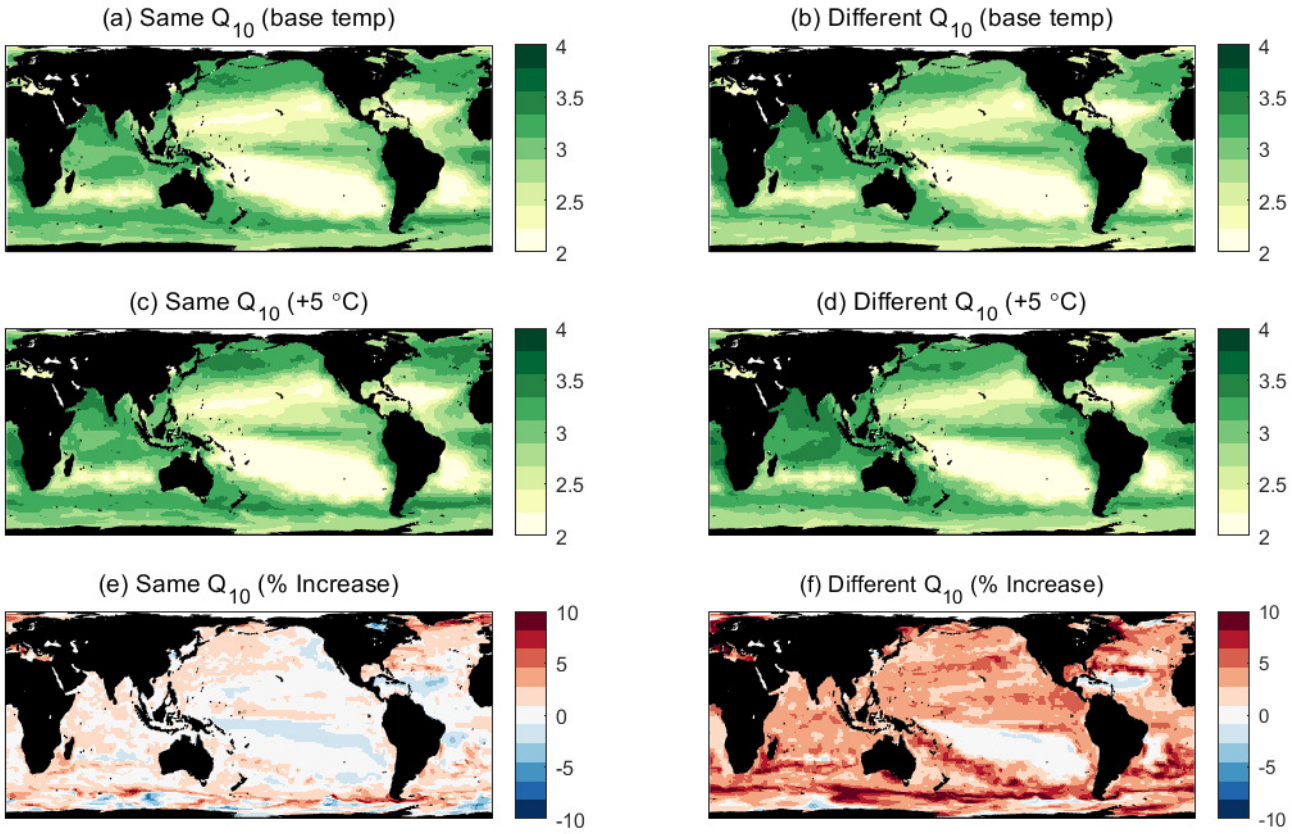

Figure 10. Global distribution of the mean food chain length under the base (a,b) and +5 degree (c,d) experiments for both Q_{10} cases and the percent difference (e,f) between the two temperature simulations.

ing results in additional export of material out of the surface ocean, resulting in ecosystems that are more productive, but contain less biomass, as the temperature increases.

Warming also broadly drives increases in mean body size in the plankton community. Interestingly, this trend is in the opposite direction of the classical thermal response of size spectra in oceanography, in which warming drives decreases in body size, that has been proposed as a universal biological response to warming (Gardner et al., 2011; Yvon-Durocher et al., 2011). Water column stratification and reduced nutrient supply are often suggested as proximate causes of this decline in mean body size (Morán et al., 2010). Here, we have ignored those factors in favor of focusing on the direct effects of temperature on metabolism. The fact that our analysis found an increase in mean body size suggests the relationship between temperature and plankton size spectra is complex, integrating multiple (possibly contradictory) mechanisms of change.

Transient dynamics were an important component of the results in this study. In the time-series simulation of the box model, productivity responded non-monotonically to an instantaneous temperature increase: NPP initially increased in response to the higher temperature, but then slowly declined as matter was removed from the system along export pathways. A similar pattern has been observed in decadal-scale changes in global NPP, which increased significantly between 1998 and 2000 and then gradually declined during the first decade of the 21st century (Behrenfeld et al., 2006). While there is not sufficient evidence to say whether the mechanism described in this paper is responsible for these patterns, the agreement between findings underscores the importance of feedbacks within the system, which can produce complex transient responses to simple changes in the drivers of the system.

Another source of complexity is the temperature sensitivities themselves. In both the Darwin and the box-model simulations, ecosystems had greater sensitivity to temperature if the Q_{10} values differed across different metabolic processes. Here, we compared the case in which all the Q_{10} values in the model are equal against the case in which the Q_{10} for heterotrophic metabolic processes is higher than that of autotrophic processes. These assumptions were based on empirical evidence that show increased temperature sensitivity in the growth rates of heterotrophs (Rose & Caron, 2007). However, our knowledge of the variability in real world Q_{10} is incomplete. Temperature sensitivity certainly varies across phytoplankton taxa (Anderson et al., 2021) and between phytoplankton and zooplankton (Eppley, 1972; Rose & Caron, 2007), but the variability in temperature sensitivity for other important ecosystem rates, including remineralization, and the regional variability across biogeochemical regimes remains largely undescribed.

Our results suggest that variability in temperature sensitivity affects the ecosystem-level thermal response of planktonic food webs. A better description of the variance in Q_{10} coefficients between different taxa and biogeochemical regimes will expand our understanding of how marine ecosystems will response to warming and should be a priority in future research. It is important to note that these temperature sensitivities are likely not fixed. Organisms adapt to their environment and evolution in response to warming temperatures may function to modulate the ecosystem response (Padfield et al., 2016). Increased thermal diversity has been shown to dampen ecosystem thermal sensitivity because communities are better able to track temperature fluctuations in the environment (Chen, 2022). A "flattening" of the Q_{10} curves via adaptation could reduce the temperature sensitivity of ecosystems and lead to smaller thermal responses.

Our study has particular relevance to Earth system models (ESMs), including those used in the IPCC CMIP ensembles. These models include Q_{10} parameterizations of temperature sensitivity for biological rates, and as such the mechanisms we describe in this study will be at play in their future change scenarios. These mechanisms such as temperature-alone driven decrease in biomass and increase in NPP will occur in their projections, but have not been isolated before. Other effects such as alterations in nutrient supplies and

light environment will occur in the ESM as well. The combination of all these stressors will lead to different outcomes in different regions (see e.g. Dutkiewicz et al., 2013). But no previous study has focused on the ecosystem-wide dyanmics as found in this study.

Darwin's sensitivity to assumptions concerning Q_{10} values may therefore also provide insight into the differences in results from various Earth system models (ESMs). There is a high degree of variability among the ESMs participating in CMIP6, with disagreement in the sign of the ecosystem response over the twenty-first century in many locations (Kwiatkowski et al., 2020). Some of this uncertainty likely arises from differences in the implementation of temperature sensitivity, varying from using the same sensitivity for all plankton types (e.g. GFDL-COBALT; Stock et al., 2020), to using different Q_{10} values for phyto- and zooplankton (e.g. IPSL-PISCES; Aumont et al., 2015), to implementing phytoplankton temperature dependent but zooplankton independent (e.g. UK-ESM-MEDUSA; Yool et al., 2013). The lack of consistency could at least partially be due to mechanisms described here. As stated earlier, these mechanisms are already at work in the CMIP6 models, albeit alongside other sources of ecosystem change. Our results could be the source of some of this uncertainty.

We have taken a diagnostic approach in our modeling method and worked to isolate one mechanism of temperature-driven ecosystem change that arises from the direct effects of temperature on metabolism. However, it is important to acknowledge that this mechanism exists in the context of a suite of direct and indirect effects that temperature has on marine food webs. These effects include changes to water column structure and stratification, changes to circulation at multiple scales, and ocean acidification (Falkowski et al., 1998; Behrenfeld et al., 2006; Martinez et al., 2009; Dutkiewicz et al., 2013, 2015, 2019). Multiple, simultaneous mechanisms of ecosystem change will alter nutrient availability, biomass, and community structure in complex ways. Ecosystem-level thermal responses are therefore an emergent behavior of a complex network of temperature-driven changes to both physics and biology in the ocean. A complete understanding of ecosystem thermal sensitivity is an iterative and ongoing process of building up layers of understanding of individual mechanisms of change and how they interact. The purpose of this study was specifically to examine the thermal response of metabolism, an effect that is present in previous models, but not fully examined.

5 Data Availability

The generic ecosystem code required to run the Darwin model is available through https://github.com/darwinproject/darwin3. The specific simulation output used in this study is available at https://dataverse.harvard.edu/dataverse/darwin (DOI will be assigned upon acceptance of the manuscript). The box model simulations are fully reproducible from the equations and parameter values included in the paper.

Acknowledgments

Work was supported by the US National Science Foundation (OCE-1851194 to HVM) and by the Simons Foundation (Award 689265 to HVM). S.D. is grateful for support from the Simons Collaboration on Computational Biogeochemical Modeling of Marine Ecosystems (CBIOMES; Simons Foundation grant 549931) and from NASA (grant 80NSSC22K0153). C.L. acknowledges support from the Swiss National Science Foundation (grant 174124). We thank Suzana Lelse, Ferdinand Pfab, and members of the Moeller lab for comments on earlier versions of this manuscript. Special thanks to Elise Cypher for scientific illustrations.

References

Anderson, S. I., Barton, A. D., Clayton, S., Dutkiewicz, S., & Rynearson, T. A.

(2021, 12). Marine phytoplankton functional types exhibit diverse responses to thermal change. *Nature Communications*, *12*, 1-9. doi: 10.1038/s41467-021-26651-8

Archibald, K. M., Dutkiewicz, S., Laufkötter, C., & Moeller, H. V. (2022). *Thermal responses in global marine planktonic food webs mediated through temperature effects on metabolism* [dataset]. DARWIN Project Dataverse. Retrieved from `https://dataverse.harvard.edu/dataverse/darwin` doi: TBD

Aumont, O., Ethé, C., Tagliabue, A., Bopp, L., & Gehlen, M. (2015, 8). Pisces-v2: An ocean biogeochemical model for carbon and ecosystem studies. *Geoscientific Model Development*, *8*, 2465-2513. doi: 10.5194/gmd-8-2465-2015

Behrenfeld, M. J., O'Malley, R. T., Siegel, D. A., McClain, C. R., Sarmiento, J. L., Feldman, G. C., ... Boss, E. S. (2006, 12). Climate-driven trends in contemporary ocean productivity. *Nature*, *444*, 752-755. doi: 10.1038/nature05317

Benedetti, F., Vogt, M., Elizondo, U. H., Righetti, D., Zimmermann, N. E., & Gruber, N. (2021, 12). Major restructuring of marine plankton assemblages under global warming. *Nature Communications*, *12*, 1-15. doi: 10.1038/s41467-021-25385-x

Bindoff, N. L., Artale, V., Cazenave, A., Gregory, J. M., Willebrand, J., Artale, V., ... Tignor, M. (2007). *Observations: oceanic climate change and sea level, in climate change 2007: the physical science basis* (S. Solomon et al., Eds.). Cambridge University Press.

Bissinger, J. E., Montagnes, D. J. S., Sharples, J., & Atkinson, D. (2008). Predicting marine phytoplankton maximum growth rates from temperature: Improving on the eppley curve using quantile regression. *Limnology and oceanography*, *53*, 487-493. Retrieved from `www.aslo.org/lo/toc/vol_53/`

Bopp, L., Aumont, O., Cadule, P., Alvain, S., & Gehlen, M. (2005, 10). Response of diatoms distribution to global warming and potential implications: A global model study. *Geophysical Research Letters*, *32*, 1-4. doi: 10.1029/2005GL023653

Bopp, L., Resplandy, L., Orr, J. C., Doney, S. C., Dunne, J. P., Gehlen, M., ... Vichi, M. (2013). Multiple stressors of ocean ecosystems in the 21st century: Projections with cmip5 models. *Biogeosciences*, *10*, 6225-6245. doi: 10.5194/bg-10-6225-2013

Boyce, D. G., Lewis, M. R., & Worm, B. (2010, 7). Global phytoplankton decline over the past century. *Nature*, *466*, 591-596. doi: 10.1038/nature09268

Buitenhuis, E. T., Vogt, M., Moriarty, R., Bednaršek, N., Doney, S. C., Leblanc, K., ... Swan, C. (2013, 7). Maredat: Towards a world atlas of marine ecosystem data. *Earth System Science Data*, *5*, 227-239. doi: 10.5194/essd-5-227-2013

Chen, B. (2022, 2). Thermal diversity affects community responses to warming. *Ecological Modelling*, *464*. doi: 10.1016/j.ecolmodel.2021.109846

Cheng, L., Abraham, J., Hausfather, Z., & Trenberth, K. E. (2019, 1). How fast are the oceans warming? *Science*, *363*, 128-129. doi: 10.1126/science.aav7619

Dutkiewicz, S., Cermeno, P., Jahn, O., Follows, M. J., Hickman, A. A., Taniguchi, D. A., & Ward, B. A. (2020, 2). Dimensions of marine phytoplankton diversity. *Biogeosciences*, *17*, 609-634. doi: 10.5194/bg-17-609-2020

Dutkiewicz, S., Hickman, A. E., Jahn, O., Henson, S., Beaulieu, C., & Monier, E. (2019, 12). Ocean colour signature of climate change. *Nature Communications*, *10*, 1-13. doi: 10.1038/s41467-019-08457-x

Dutkiewicz, S., Morris, J. J., Follows, M. J., Scott, J., Levitan, O., Dyhrman, S. T., & Berman-Frank, I. (2015, 11). Impact of ocean acidification on the structure of future phytoplankton communities. *Nature Climate Change*, *5*, 1002-1006. doi: 10.1038/nclimate2722

Dutkiewicz, S., Scott, J. R., & Follows, M. J. (2013, 6). Winners and losers: Ecological and biogeochemical changes in a warming ocean. *Global Biogeochemical Cycles*, *27*, 463-477. doi: 10.1002/gbc.20042

Eppley, R. W. (1972). Temperature and phytoplankton growth in the sea. *Fishery Bulletin*, *70*, 1063-1085.

Falkowski, P. G., Barber, R. T., & Smetacek, V. (1998). Biogeochemical controls and feedbacks on ocean primary production. *Science*, *281*, 200-2006. Retrieved from `https://www.science.org`

Follett, C. L., Dutkiewicz, S., Ribalet, F., Zakem, E., Caron, D., Armbrust, E. V., & Follows, M. J. (2022). Trophic interactions with heterotrophic bacteria limit the range of prochlorococcus. *Proceedings of the National Academy of Sciences*, *119*. doi: 10.1073/pnas.2110993118/-/DCSupplemental

Frölicher, T. L., Fischer, E. M., & Gruber, N. (2018, 8). Marine heatwaves under global warming. *Nature*, *560*, 360-364. doi: 10.1038/s41586-018-0383-9

Gardner, J. L., Peters, A., Kearney, M. R., Joseph, L., & Heinsohn, R. (2011, 6). Declining body size: A third universal response to warming? *Trends in Ecology and Evolution*, *26*, 285-291. doi: 10.1016/j.tree.2011.03.005

Geider, R. J., Maclntyre, H. L., & Kana, T. M. (1998). A dynamic regulatory model of phytoplanktonic acclimation to light, nutrients, and temperature. *Limnology and oceanography*, *43*, 679-694.

Hansen, P. J., Bjørnsen, P. K., & Hansen, B. W. (1997). Zooplankton grazing and growth: Scaling within the 2-2,000-um body size range. *Limnology and oceanography*, *42*, 687-704.

Henson, S. A., Sarmiento, J. L., Dunne, J. P., Bopp, L., Lima, I., Doney, S. C., ... Beaulieu, C. (2010). Detection of anthropogenic climate change in satellite records of ocean chlorophyll and productivity. *Biogeosciences*, *7*, 621-640. Retrieved from `www.biogeosciences.net/7/621/2010/`

Holling, C. S. (1965). The functional response of predators to prey density and its role in mimicry and population regulation. *Memoirs of the Entomological Society of Canada*, *97*, 5-60. doi: 10.4039/entm9745fv

Irwin, A. J., & Oliver, M. J. (2009, 9). Are ocean deserts getting larger? *Geophysical Research Letters*, *36*. doi: 10.1029/2009GL039883

Kiørboe, T. (2018). *A mechanistic approach to plankton ecology.* Princeton University Press.

Kwiatkowski, L., Torres, O., Bopp, L., Aumont, O., Chamberlain, M., Christian, J. R., ... Ziehn, T. (2020, 7). Twenty-first century ocean warming, acidification, deoxygenation, and upper-ocean nutrient and primary production decline from cmip6 model projections. *Biogeosciences*, *17*, 3439-3470. doi: 10.5194/bg-17-3439-2020

Laufkotter, C., Vogt, M., Gruber, N., Aita-Noguchi, M., Aumont, O., Bopp, L., ... Volker, C. (2015, 12). Drivers and uncertainties of future global marine primary production in marine ecosystem models. *Biogeosciences*, *12*, 6955-6984. doi: 10.5194/bg-12-6955-2015

Laufkötter, C., Zscheischler, J., & Frölicher, T. L. (2020). High-impact marine heatwaves attributable to human-induced global warming. *Science*, *369*, 1621-1625. Retrieved from `https://www.science.org`

López-Urrutia, A. A., Martin, E. S., Harris, R. P., & Irigoien, X. (2006). Scaling the metabolic balance of the oceans. *Proceedings of the National Academy of Sciences*, *103*, 8739-8744. Retrieved from `www.pnas.orgcgidoi10.1073pnas.0601137103`

Marshall, J., Adcroft, A., Hill, C., Perelman, L., & Heisey, C. (1997). A finite-volume, incompressible navier stokes model for, studies of the ocean on parallel computers. *Journal of Geophysical Research C: Oceans*, *102*, 5753-5766. doi: 10.1029/96JC02775

Martinez, E., Antoine, D., & Gentili, B. (2009). Climate-driven basin-scale decadal oscillations of oceanic phytoplankton. *Science*, *326*, 1253-1256. Retrieved from `https://www.science.org`

Morán, X. A. G., Ángel López-Urrutia, Calvo-Díaz, A., & LI, W. K. (2010). Increas-

ing importance of small phytoplankton in a warmer ocean. *Global Change Biology*, *16*, 1137-1144. doi: 10.1111/j.1365-2486.2009.01960.x

Murphy, G. E., Romanuk, T. N., & Worm, B. (2020). Cascading effects of climate change on plankton community structure. *Ecology and Evolution*, *10*, 2170-2181. doi: 10.1002/ece3.6055

Padfield, D., Yvon-Durocher, G., Buckling, A., Jennings, S., & Yvon-Durocher, G. (2016, 2). Rapid evolution of metabolic traits explains thermal adaptation in phytoplankton. *Ecology Letters*, *19*, 133-142. doi: 10.1111/ele.12545

Polovina, J. J., Howell, E. A., & Abecassis, M. (2008, 2). Ocean's least productive waters are expanding. *Geophysical Research Letters*, *35*. doi: 10.1029/2007GL031745

Rose, J. M., & Caron, D. A. (2007). Does low temperature constrain the growth rates of heterotrophic protists? evidence and implications for algal blooms in cold waters. *Limnology and Oceanography*, *52*, 886-895. Retrieved from `http://www.aslo.org/lo/toc/vol_52/`

Schartau, M., Landry, M. R., & Armstrong, R. A. (2010, 8). Density estimation of plankton size spectra: A reanalysis of ironex ii data. *Journal of Plankton Research*, *32*, 1167-1184. doi: 10.1093/plankt/fbq072

Stock, C. A., Dunne, J. P., Fan, S., Ginoux, P., John, J., Krasting, J. P., ... Zadeh, N. (2020, 10). Ocean biogeochemistry in gfdl's earth system model 4.1 and its response to increasing atmospheric co2. *Journal of Advances in Modeling Earth Systems*, *12*. doi: 10.1029/2019MS002043

Taucher, J., & Oschlies, A. (2011, 1). Can we predict the direction of marine primary production change under global warming? *Geophysical Research Letters*, *38*. doi: 10.1029/2010GL045934

Thomas, M. K., Kremer, C. T., Klausmeier, C. A., & Litchman, E. (2012). A global pattern of thermal adaptation in marine phytoplankton. *Science*, *338*, 1085-1088. Retrieved from `https://www.science.org`

Ward, B. A. (2015, 8). Temperature-correlated changes in phytoplankton community structure are restricted to polar waters. *PLoS ONE*, *10*. doi: 10.1371/journal.pone.0135581

Westerling, A. L., Hidalgo, H. G., Cayan, D. R., & Swetnam, T. W. (2006, 8). Warming and earlier spring increase western u.s. forest wildfire activity. *Science*, *313*, 940-943. doi: 10.1126/science.1128834

Wunsch, C., & Heimbach, P. (2007). Practical global oceanic state estimation. *Physica D: Nonlinear Phenomena*, *230*, 197-208. doi: 10.1016/j.physd.2006.09.040

Yool, A., Popova, E. E., & Anderson, T. R. (2013). Medusa-2.0: An intermediate complexity biogeochemical model of the marine carbon cycle for climate change and ocean acidification studies. *Geoscientific Model Development*, *6*, 1767-1811. doi: 10.5194/gmd-6-1767-2013

Yvon-Durocher, G., Montoya, J. M., Trimmer, M., & Woodward, G. (2011, 4). Warming alters the size spectrum and shifts the distribution of biomass in freshwater ecosystems. *Global Change Biology*, *17*, 1681-1694. doi: 10.1111/j.1365-2486.2010.02321.x